



Cite this: *Chem. Sci.*, 2020, **11**, 1698

All publication charges for this article have been paid for by the Royal Society of Chemistry

Received 29th November 2019

Accepted 1st January 2020

DOI: 10.1039/c9sc06047b

rsc.li/chemical-science

Biomimetic O₂ adsorption in an iron metal–organic framework for air separation†

Douglas A. Reed, ^a Dianne J. Xiao, ^a Henry Z. H. Jiang, ^a Khetpakorn Chakarawet, ^a Julia Oktawiec ^a and Jeffrey R. Long ^{a,b,c}

Bio-inspired motifs for gas binding and small molecule activation can be used to design more selective adsorbents for gas separation applications. Here, we report an iron metal–organic framework, Fe-BTTri ($\text{Fe}_3[(\text{Fe}_4\text{Cl})_3(\text{BTTri})_8]_2 \cdot 18\text{CH}_3\text{OH}$, $\text{H}_3\text{BTTri} = 1,3,5\text{-tris}(1H-1,2,3\text{-triazol-5-yl})\text{benzene}$), that binds O₂ in a manner similar to hemoglobin and therefore results in highly selective O₂ binding. As confirmed by gas adsorption studies and Mössbauer and infrared spectroscopy data, the exposed iron sites in the framework reversibly adsorb substantial amounts of O₂ at low temperatures by converting between high-spin, square-pyramidal Fe(II) centers in the activated material to low-spin, octahedral Fe(III)–superoxide sites upon gas binding. This change in both oxidation state and spin state observed in Fe-BTTri leads to selective and readily reversible O₂ binding, with the highest reported O₂/N₂ selectivity for any iron-based framework.

Introduction

Metal–organic frameworks (MOFs) are a class of permanently porous solids built using organic linkers and inorganic nodes^{1–3} that have been studied for a wide variety of applications including catalysis⁴ and gas separations.⁵ The inherent tunability of metal–organic frameworks has made it possible to design structures with bio-inspired pores precisely engineered for applications in catalysis^{6,7} and cooperative substrate binding.^{8,9} The study of biomimetic gas binding to metal sites, a broad topic in the field of inorganic chemistry as a whole,^{10–14} can also be applied to gas adsorption and gas separations in porous frameworks.^{8,15–17} However, successful implementation of this strategy is somewhat challenging, as the highly specific metal–ligand bonds required for such model systems are difficult to engineer in sufficient densities to afford reasonable separation capacities, thus limiting their effectiveness as adsorbents. One process that would benefit from biomimetic gas binding is the industrial separation of air for the production of high-purity O₂, which is widely used for chemical synthesis, chemical processing, and the implementation of oxyfuel

combustion.^{18,19} Industrial air separation, dominated by the separation of O₂ and N₂, is primarily accomplished through energetically demanding cryogenic distillation; current adsorbent-based technologies, which are predominantly N₂-selective, are not competitive at large scales.²⁰ In contrast, biological systems perform air separations by selectively and reversibly binding O₂ through various electronic transformations at transition metal binding sites, using carriers such as hemoglobin, hemocyanin, and hemerythrin.²¹ For example, the square pyramidal, high-spin Fe(II) heme centers in hemoglobin selectively bind O₂ by undergoing both an oxidation and a spin state transition to form octahedral, low-spin Fe(III)–superoxide species. Replicating such selective binding mechanisms found in proteins is one intriguing strategy toward the design of more effective adsorbents for O₂/N₂ separations.

Metal–organic frameworks bearing redox-active open metal sites have been investigated for the adsorption of O₂,^{22–28} and the framework Fe₂(dobdc) (dobdc^{4–} = 2,5-dioxido-1,4-benzenedicarboxylate) reversibly binds O₂ at low temperatures *via* charge transfer from exposed Fe(II) sites.²³ However, below -50°C the weak ligand field afforded by the framework linkers leads to only partial charge transfer to O₂, generating high-spin iron sites with an oxidation state between Fe(II) and Fe(III). This Fe–O₂ interaction is much weaker than that found in heme systems, and while the framework O₂/N₂ selectivities are much higher than traditional adsorbents studied for air separations,²⁰ the selectivity could be further improved for practical applications. The framework PCN-224Fe, which features Fe(II) heme centers, can transform from an intermediate-spin, four-coordinate Fe(II) in the activated phase to a low-spin, five-coordinate superoxide-bound Fe(III) upon O₂ adsorption, but

^aDepartment of Chemistry, University of California, Berkeley, CA 94720, USA. E-mail: jrlong@berkeley.edu

^bDepartment of Chemical Engineering, University of California, Berkeley, CA 94720, USA

^cMaterials Sciences Division, Lawrence Berkeley National Lab, Berkeley, CA 94720, USA

† Electronic supplementary information (ESI) available: Full experimental details, additional gas adsorption data and analysis, additional characterization data and analysis (Mössbauer spectroscopy, infrared spectroscopy, powder X-ray diffraction), and supplementary discussion. See DOI: 10.1039/c9sc06047b



the O_2 capacity needs to be improved for separation purposes.¹⁵ A structurally flexible metal-organic framework with an electron-donating ligand environment would support the iron site electronic changes observed with O_2 binding in hemoglobin, and combined with a high concentration of Fe(II) sites could consequently exhibit improved O_2/N_2 selectivities and capacities.

Recently, we reported the material Fe-BTTri ($Fe_3[(Fe_4Cl)_3(-BTTri)_8]_2 \cdot 18CH_3OH$, $H_3BTTri = 1,3,5$ -tris($1H$ -1,2,3-triazol-5-yl)benzene), which features Fe(II) centers bound in an environment similar to hemoglobin iron sites.²⁹ This framework has been shown to accommodate both high- and low-spin iron centers, making it an excellent candidate to study the various electronic transformations required in biomimetic O_2 binding. Here, we demonstrate that Fe-BTTri can indeed undergo an electronic transformation similar to that of hemoglobin upon binding oxygen, resulting in O_2/N_2 selectivities that are substantially higher than other iron-based adsorbents.

Results and discussion

The framework Fe-BTTri was synthesized and activated according to a previously reported procedure.²⁹ Similar to hemoglobin, the material features five-coordinate iron centers in a square pyramidal geometry, with equatorial sites occupied by N-atom heterocyclic donor ligands and an open coordination site for O_2 binding (Fig. 1). Previous structural, spectroscopic, and magnetic studies of Fe-BTTri have shown that the high-spin Fe(II) sites in the activated phase are present in sufficiently high density to allow for large gas adsorption capacities.²⁹ The material is irreversibly oxidized upon exposure to air, but similar to $Fe_2(dobdc)$, the O_2 adsorption is selective and reversible under more controlled, anhydrous conditions.²³

The O_2 adsorption isotherm for Fe-BTTri collected at $-78\text{ }^\circ\text{C}$ features an initial steep rise to a capacity of 1.2 mmol g^{-1} at just $100\text{ }\mu\text{bar}$ followed by a more gradual increase to a capacity of 5.9 mmol g^{-1} at 1 bar (Fig. 2). Importantly, at 210 mbar , corresponding to the partial pressure of O_2 in air, the adsorption capacity is a substantial 3.3 mmol g^{-1} , or approximately 10 wt\% of O_2 , highlighting the potential of this material for practical separations. This capacity corresponds to adsorption of O_2 at 80% of the framework iron sites (excluding charge balancing extra-framework Fe(II) cations). At this temperature, powder crystalline samples of the material remain highly crystalline when exposed to O_2 (Fig. S6†). Moreover, the powder X-ray diffraction (PXRD) data show that the unit cell volume decreases relative to the bare framework, indicative of a structural contraction upon O_2 adsorption (Fig. S6†).

We first turned to Mössbauer spectroscopy to investigate a possible iron redox or spin state transition following exposure of Fe-BTTri to O_2 . Previous studies of the activated framework yielded isomer shift values (δ) ranging from 1.05 – 1.07 mm s^{-1} and quadrupole splitting values (ΔE_Q) from 1.80 – 3.06 mm s^{-1} .²⁹ The slightly different iron environments giving rise to these values can be ascribed to the presence of disordered, charge-balancing extra-framework cations as well as residual solvent molecules remaining upon activation, which has also been seen

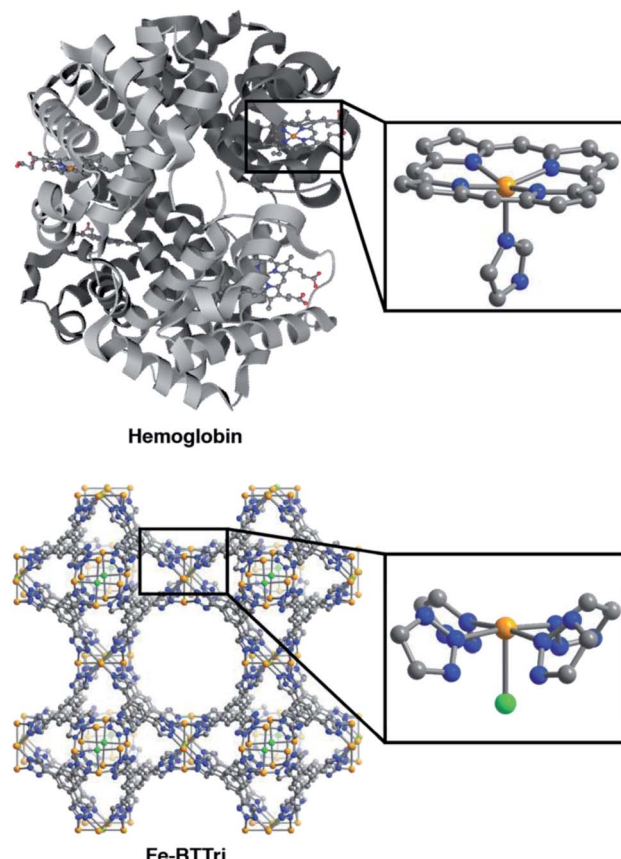


Fig. 1 Structures of hemoglobin (top)⁴² and Fe-BTTri (bottom),²⁹ with expanded views of the individual iron coordination environments in each material. Orange, grey, blue, red, and green spheres represent Fe, C, N, O, and Cl atoms, respectively; H-atoms and solvent molecules are omitted for clarity.

in the structurally analogous framework Fe-BTT ($Fe_3[(Fe_4Cl)_3(-BTT)_8(CH_3OH)_4]_2$, $BTT^{3-} = 1,3,5$ -benzenetristetrazolate).³⁰ Dosing activated Fe-BTTri with 210 mbar of O_2 at $-78\text{ }^\circ\text{C}$

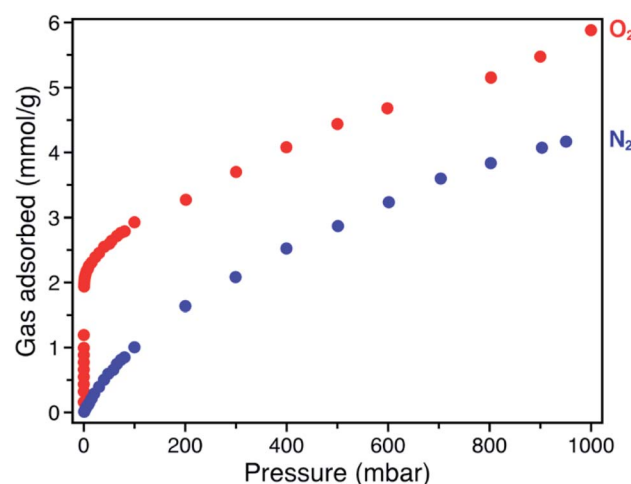


Fig. 2 Gas adsorption isotherms of O_2 (red) and N_2 (blue), collected at $-78\text{ }^\circ\text{C}$ for Fe-BTTri.



resulted in the appearance of several new Mössbauer spectral features (Fig. 3). The dominant feature ($\delta = 0.309(2)$ mm s^{-1} , $\Delta E_Q = 2.370(3)$ mm s^{-1}) comprises 50.8(9)% of the total absorption area and is consistent with low-spin, octahedrally-coordinated Fe(III), which typically exhibit quadrupole splitting values >2 mm s^{-1} .³¹ This result is the first example of an iron site in a metal-organic framework converting from high-spin Fe(II) to low-spin Fe(III) upon adsorbate binding. Importantly, these Mössbauer parameters also closely align with those obtained for oxyhemoglobin and biomimetic iron porphyrin-O₂ compounds.^{32,33} The remaining spectral features are attributed to residual high-spin Fe(II) in extra-framework and framework sites, which is expected based on the gas sorption data. A small amount of high-spin Fe(III) impurity is also observed due to sample warming (see the Discussion in the ESI† for additional details).

The nature of the bound dioxygen molecule was also investigated *via* *in situ* infrared spectroscopy, using a custom-built DRIFTS setup (Fig. S7†). Cooling a sample of Fe-BTTri to -78 °C and dosing with 15 mbar of $^{16}\text{O}_2$ resulted in the appearance of a new stretch at 1199 cm $^{-1}$ that shifts to 1136 cm $^{-1}$ with isotopically labeled $^{18}\text{O}_2$. Given that several of the framework peaks change upon O₂ binding, the spectrum of the $^{18}\text{O}_2$ -dosed material was subtracted from that of the $^{16}\text{O}_2$ -dosed framework to isolate the O₂-based vibrations. The difference spectrum confirms that the peaks at 1136 and 1199 cm $^{-1}$ arise from the O–O stretch. The resonance at 1199 cm $^{-1}$ is characteristic of a superoxo (O₂ $^-$) species, which typically show infrared stretching frequencies between 1070 – 1200 cm $^{-1}$,³⁴ and is similar to stretching frequencies observed for O₂ in oxyhemoglobin and other model systems.^{35,36}

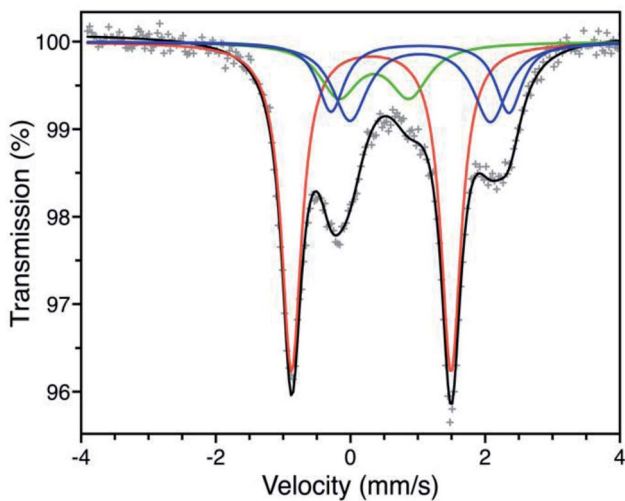


Fig. 3 Mössbauer spectrum of Fe-BTTri collected at -78 °C under a 210 mbar atmosphere of O₂. Experimental data are shown as grey plusses and the total fit is shown in black. The red component is assigned to low-spin Fe(III) centers bound to O₂ $^-$, the green component to a high-spin Fe(III) decomposition product, and the blue components to high-spin Fe(II) species at framework and extra-framework sites. The ESI† contains spectral parameters for all sites (Table S3†), along with supplemental discussion of the green and blue components.

To further probe the interaction between the iron centers and O₂, gas adsorption isotherms were collected at various temperatures and analyzed to determine the Fe–O₂ binding enthalpy, or isosteric heat of adsorption. Isotherm data collected at -78 , -61 , and -49 °C were fit to a dual-site Langmuir–Freundlich equation (Fig. S1†), and the Clausius–Clapeyron relation was used to calculate an isosteric heat of adsorption of -51 kJ mol $^{-1}$ (Fig. S4†). This value is similar to those reported for O₂ binding in heme systems, which typically range from -52 to -62 kJ mol $^{-1}$.^{19,37} Additionally, when compared to the value of -41 kJ mol $^{-1}$ obtained for O₂ binding in Fe₂(dobdc),²³ it is clear the different binding mechanism in Fe-BTTri facilitates substantially stronger iron–O₂ interactions. Indeed, among frameworks exhibiting fully reversible O₂ adsorption,^{15,23,24,26} Fe-BTTri shows the highest binding affinity for O₂.

The similar O₂ binding in Fe-BTTri and heme systems suggests that Fe-BTTri should perform selective and reversible O₂ binding. Low-temperature cycling experiments revealed that O₂ binding in Fe-BTTri is fully reversible, and the material can be completely regenerated under mild conditions with very small temperature swings (Fig. 4). Heating O₂-bound Fe-BTTri to -40 °C under vacuum for just 30 minutes fully regenerates the material, leading to an identical O₂ uptake at 210 mbar compared to that of the pristine material over five cycles. Variable-temperature Mössbauer spectra collected under 210 mbar of O₂ similarly show that >80% of the O₂ bound to low-spin Fe(III) is released upon warming the sample from -78 to -28 °C (Fig. S8†). Finally, variable-temperature PXRD data collected on a framework sample dosed with 7 mbar of O₂ show fully reversible unit cell volume contractions and expansions over multiple cycles between -80 and -30 °C, consistent with the reversible binding and release of O₂ (Fig. S6†). We note that above -15 °C, adsorption of O₂ becomes irreversible.

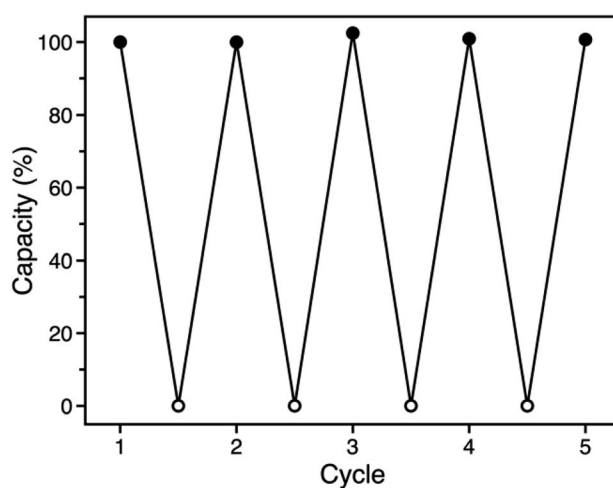


Fig. 4 Cycling data for successive adsorption and desorption of O₂ in Fe-BTTri, expressed as a percentage of the capacity measured for cycle 1. Adsorption (solid symbols) occurred within 10 minutes upon dosing O₂ at 210 mbar and -78 °C, and complete desorption (open symbols) was accomplished by warming the sample to -40 °C under dynamic vacuum for 30 minutes.



Ultimately, the combined oxidation and spin state transition observed for Fe-BTTri enables highly selective and reversible low-temperature adsorption of O₂.

The O₂/N₂ selectivity of Fe-BTTri for air separation applications was assessed from analysis of O₂ and N₂ gas adsorption data (Fig. 2). In comparison to that of O₂, the N₂ adsorption curve rises much more gradually, and at all measured pressures Fe-BTTri adsorbs significantly more O₂ than N₂. Furthermore, the isosteric heat of adsorption for N₂ is only -14 kJ mol^{-1} , substantially smaller in magnitude than that measured for O₂ (Fig. S4†). Ideal Adsorbed Solution Theory (IAST) was used to quantify the framework O₂/N₂ selectivity from the single component isotherms. For 21% O₂ in N₂ at a total pressure of 1 bar, which approximates the composition of air, Fe-BTTri shows an IAST selectivity value of 27 at $-78\text{ }^\circ\text{C}$, which corresponds to 88% pure O₂ in the adsorbed phase. This value is the highest reported for any iron-based framework. For comparison, Fe₂(dobdc) displays an IAST selectivity value of approximately 11 under similar conditions.²³ Additionally, the binding enthalpy of all other gaseous components of air, such as CO₂, are significantly smaller in magnitude than that of O₂ and should not affect the O₂/N₂ selectivity.²⁹ This is another important contrast to Fe₂(dobdc), where CO₂ adsorbs with a similar binding affinity to that of O₂ and may impact the O₂ selectivity performance in air separations.³⁸

Interestingly, the O₂/N₂ IAST selectivity values for Fe-BTTri remain relatively constant over a wide temperature range. For the 21% O₂ in N₂ mixture, the selectivity increases to 31 when the temperature is increased to $-61\text{ }^\circ\text{C}$, and even at $-49\text{ }^\circ\text{C}$ the selectivity remains high at 28. An increase in selectivity with temperature has been found for other separations involving adsorbate-induced spin state transitions,²⁹ but this result is in stark contrast to that for other O₂ adsorbents, which exhibit diminished selectivity with increasing temperature.^{23,24} For example, the selectivity of Fe₂(dobdc) decreases by over 30%, from 11 to 7.5, over a much smaller temperature range of -72 to $-59\text{ }^\circ\text{C}$.²³ The ability of redox and spin state flexible adsorbents to remain selective at higher temperatures is another advantage of this binding mechanism. To the best of our knowledge, this is the first example of temperature-independent selectivity in O₂-selective adsorbents.

Lastly, we examined the potential utility of this material for O₂-scrubbing applications, as O₂ is a potential poison for several N₂ fixation catalysts.³⁹ The O₂ capacity of Fe-BTTri is approximately 1.2 mmol g⁻¹ at just 100 ppm, corresponding to a removal capacity of nearly 4 wt% at low O₂ partial pressures (Fig. S3†). In comparison, the adsorption capacity of Fe₂(dobdc) at these temperatures and pressures is approximately 0.2 mmol g⁻¹.²³ Importantly, due to its steep O₂ adsorption isotherm profile, Fe-BTTri is also highly selective for O₂ at low O₂ partial pressures (Fig. S5†). Analysis of the IAST selectivity values for varying O₂/N₂ compositions at 1 bar total pressure and $-78\text{ }^\circ\text{C}$ revealed that the selectivity increases at lower O₂ concentrations, reaching a value of 68 for a 5% O₂ in N₂ mixture. This result is again in contrast to other materials,²³ for which the selectivity remains constant or even decreases at low O₂ concentrations, and demonstrates that Fe-BTTri is promising for both air separation and O₂-scrubbing applications.

Conclusions

The results shown here demonstrate that materials exhibiting new mechanisms for metal-site gas binding can be achieved using inspiration from biology. In particular, the framework Fe-BTTri, featuring iron sites structurally similar to heme iron, shows high selectivities for O₂ over N₂ for a range of temperatures and pressures. The highly tunable nature of metal-organic frameworks should enable the design and installation of other bio-inspired motifs, such as pendant hydrogen bond donors *via* secondary coordination sphere modification,⁴⁰ bimetallic O₂ binding sites using neighboring metal centers capable of synergistic binding,^{7,41} and cooperative adsorption sites.⁹ These approaches may afford new means of binding and activating gaseous substrates and serve as models for the continued development of advanced adsorbents.

Conflicts of interest

The authors declare the following competing financial interests: J. R. L. has a financial interest in Mosaic Materials, Inc., a startup company working to commercialize metal-organic frameworks for gas separations. The University of California, Berkeley has applied for a patent on some of the materials discussed herein, on which J. R. L. and D. A. R. are listed as inventors.

Acknowledgements

This work was supported by the U.S. Department of Energy, Office of Science, Office of Basic Energy Sciences under Award DE-SC0019992. Powder X-ray diffraction data were collected at Beamline 17-BM at the Advanced Photon Source, a DOE Office of Science User Facility, operated by Argonne National Laboratory under contract DE-AC02-06CH11357. We thank the National Science Foundation for graduate fellowship support of D. A. R., D. J. X., and J. O., and thank Dr K. R. Meihaus for editorial assistance.

Notes and references

- 1 O. M. Yaghi, H. Li, M. Eddaoudi and M. O'Keefe, *Nature*, 1999, **402**, 276.
- 2 S. Kitagawa, R. Kitaura and S.-I. Noro, *Angew. Chem., Int. Ed.*, 2004, **43**, 2334.
- 3 G. Ferey, *Chem. Soc. Rev.*, 2008, **37**, 191.
- 4 J.-R. Li, R. J. Kuppler and H.-C. Zhou, *Chem. Soc. Rev.*, 2009, **38**, 1477.
- 5 J. Lee, O. K. Farha, J. Roberts, K. A. Scheidt, S. T. Nguyen and J. R. Hupp, *Chem. Soc. Rev.*, 2009, **38**, 1450.
- 6 Z.-Y. Gu, J. Park, A. Raiff, Z. Wei and H.-C. Zhou, *ChemCatChem*, 2014, **6**, 67.
- 7 D. Y. Osadchii, A. I. Olivos-Suarez, Á. Szécsényi, G. Li, M. A. Nasalevich, I. A. Dugulan, P. S. Crespo, E. J. M. Hensen, S. L. Veber, M. V. Fedin, G. Sankar, E. A. Pidko and J. Gascon, *ACS Catal.*, 2018, **8**, 5542.



8 T. M. McDonald, J. A. Mason, X. Kong, E. D. Bloch, D. Gygi, A. Dani, V. Crocella, F. Giordanino, S. O. Odoh, W. Drisdell, B. Vlaisavljevich, A. L. Dzubak, R. Poloni, S. K. Schnell, N. Planas, K. Lee, T. Pascal, L. F. Wan, D. Prendergast, J. B. Neaton, B. Smit, J. B. Kortright, L. Gagliardi, S. Bordiga, J. A. Reimer and J. R. Long, *Nature*, 2015, **519**, 303.

9 D. A. Reed, B. K. Keitz, J. Oktawiec, J. A. Mason, T. Runčevski, D. J. Xiao, L. E. Darago, V. Crocella, S. Bordiga and J. R. Long, *Nature*, 2017, **550**, 96.

10 J. P. Collman, J. I. Brauman and K. S. Suslick, *J. Am. Chem. Soc.*, 1975, **97**, 7185.

11 J. P. Collman, J. I. Brauman, E. Rose and K. S. Suslick, *Proc. Natl. Acad. Sci. U. S. A.*, 1978, **75**, 1052.

12 C. Citek, S. Herres-Pawlis and T. D. P. Stack, *Acc. Chem. Res.*, 2015, **48**, 2424.

13 W. B. Tolman, *Acc. Chem. Res.*, 1997, **30**, 227.

14 T. J. Mizoguchi and S. J. Lippard, *J. Am. Chem. Soc.*, 1998, **120**, 11022.

15 J. S. Anderson, A. T. Gallagher, J. A. Mason and T. D. Harris, *J. Am. Chem. Soc.*, 2014, **136**, 16489.

16 A. M. Wright, Z. Wu, G. Zhang, J. L. Mancuso, R. J. Comito, R. W. Day, C. H. Hendon, J. T. Miller and M. Dinca, *Chem.*, 2018, **4**, 2894.

17 C. E. Bien, K. K. Chen, S.-C. Chien, B. R. Riener, L.-C. Lin, C. R. Wade and W. S. W. Ho, *J. Am. Chem. Soc.*, 2018, **140**, 12662.

18 N. N. Greenwood and A. Earnshaw, *Chemistry of the Elements*, Butterworth Heinemann, Burlington, MA, 2nd edn, 2002.

19 M. J. Kirschner, A. Alekseev, S. Dowy, M. Grahl, L. Jansson, P. Keil, G. Lauermann, M. Meilinger, W. Schmehl, H. Weckler and C. Windmeier, Oxygen, in *Ullmann's Encyclopedia of Industrial Chemistry*, Wiley-VCH, Weinheim, 2017.

20 A. R. Smith and J. Klosek, *Fuel Process. Technol.*, 2001, **70**, 115.

21 K. Imai, Oxygen-Binding Proteins, in *Encyclopedia of Molecular Biology*, John Wiley and Sons, 2002.

22 L. J. Murray, M. Dincă, J. Yano, S. Chavan, S. Bordiga, C. M. Brown and J. R. Long, *J. Am. Chem. Soc.*, 2010, **132**, 7856.

23 E. D. Bloch, L. J. Murray, W. L. Queen, S. Chavan, S. N. Maximoff, J. P. Bigi, R. Krishna, V. K. Peterson, F. Grandjean, G. J. Long, B. Smit, S. Bordiga, C. M. Brown and J. R. Long, *J. Am. Chem. Soc.*, 2011, **133**, 14814.

24 D. J. Xiao, M. I. Gonzalez, L. E. Darago, K. D. Vogiatzis, E. Haldoupis, L. Gagliardi and J. R. Long, *J. Am. Chem. Soc.*, 2016, **138**, 7161.

25 E. D. Bloch, W. L. Queen, M. R. Hudson, J. A. Mason, D. J. Xiao, L. J. Murray, R. Flacau, C. M. Brown and J. R. Long, *Angew. Chem., Int. Ed.*, 2016, **55**, 8605.

26 A. T. Gallagher, J. Y. Lee, V. Kathiresan, J. S. Anderson, B. M. Hoffman and T. D. Harris, *Chem. Sci.*, 2018, **9**, 1596.

27 A. T. Gallagher, M. L. Kelty, J. G. Park, J. S. Anderson, J. A. Mason, J. P. S. Walsh, S. L. Collins and T. D. Harris, *Inorg. Chem. Front.*, 2016, **3**, 536.

28 D. Denysenko, M. Grzywa, J. Jelic, K. Reuter and D. Volkmer, *Angew. Chem., Int. Ed.*, 2014, **53**, 5832.

29 D. A. Reed, D. J. Xiao, M. I. Gonzalez, L. E. Darago, Z. R. Herm, F. Grandjean and J. R. Long, *J. Am. Chem. Soc.*, 2016, **138**, 5594.

30 K. Sumida, S. Horike, S. S. Kaye, Z. R. Herm, W. L. Queen, C. M. Brown, F. Grandjean, G. J. Long, A. Dailly and J. R. Long, *Chem. Sci.*, 2010, **1**, 184.

31 P. Gütlich, E. Bill and A. X. Trautwein, *Mossbauer Spectroscopy and Transition Metal Chemistry*, Springer-Verlag, Berlin, 2007.

32 Y. Maeda, T. Harami, Y. Morita, A. Trautwein and U. Gonser, *J. Chem. Phys.*, 1981, **75**, 36.

33 K. Spartalian, G. Lang, J. P. Collman, R. R. Gagne and C. A. Reed, *J. Chem. Phys.*, 1975, **63**, 5375.

34 R. D. Jones, D. A. Summerville and F. Basolo, *Chem. Rev.*, 1979, **79**, 139.

35 C. H. Barlow, J. C. Maxwell, W. J. Wallace and W. S. Caughey, *Biochem. Biophys. Res. Commun.*, 1973, **55**, 91.

36 C. A. Reed and S. K. Cheung, *Proc. Natl. Acad. Sci. U. S. A.*, 1977, **74**, 1780.

37 E. C. Neiderhoffer, J. H. Timmons and A. E. Martell, *Chem. Rev.*, 1984, **84**, 137.

38 W. L. Queen, M. R. Hudson, E. D. Bloch, J. A. Mason, M. I. Gonzalez, J. S. Lee, D. Gygi, J. D. Howe, K. Lee, T. A. Darwish, M. James, V. K. Peterson, S. J. Teat, B. Smit, J. B. Neaton, J. R. Long and C. M. Brown, *Chem. Sci.*, 2014, **5**, 4569.

39 K. C. Waugh, D. Butler and B. E. Harden, *Catal. Lett.*, 1994, **24**, 197.

40 D. J. Xiao, J. Oktawiec, P. J. Milner and J. R. Long, *J. Am. Chem. Soc.*, 2016, **138**, 14371.

41 M. I. Gonzalez, M. T. Kapelewski, E. D. Bloch, P. J. Milner, D. A. Reed, M. R. Hudson, J. A. Mason, G. Barin, C. M. Brown and J. R. Long, *J. Am. Chem. Soc.*, 2018, **140**, 3412.

42 S.-Y. Park, T. Yokoyama, N. Shibayama, Y. Shiro and J. R. H. Tame, *J. Mol. Biol.*, 2006, **360**, 690.

